Ti NANOPARTICLES: DISLOCATION IDENTIFICATION AND STRUCTURAL ANALYSIS

Lucia BAJTOŠOVÁ[1], Nikoleta ŠTAFFENOVÁ[1], Elena CHOCHOĽAKOVÁ[1], Jan HANUŠ[1], Jan FIKAR[2], Miroslav CIESLAR[1]

[1]*Charles University, Faculty of Mathematics and Physics, Prague, Czech Republic, EU, 96473937@o365.cuni.cz, nikoleta.staffenova635@student.cuni.cz, ech4285@gmail.com, Jan.Hanus@mff.cuni.cz, Miroslav.Cieslar@mff.cuni.cz*

[2]*Czech Academy of Sciences, Institute of Physics of Materials, Brno, Czech Republic, EU, fikar@ipm.cz*

https://doi.org/10.37904/metal.2024.4965

Abstract

Titanium nanoparticles are renowned for their high strength-to-weight ratio, excellent corrosion resistance, and biocompatibility, making them promising for various advanced applications. This study explores the properties of Ti nanoparticles, mainly focusing on dislocation analysis. We utilize advanced transmission electron microscopy techniques, including high-resolution TEM and energy dispersive spectroscopy, to investigate the dislocations in Ti nanoparticles produced by magnetron sputtering. The nanoparticles exhibit a hexagonal close-packed (hcp) structure with a TiO-oxidized shell. The analysis of dislocation Burgers vectors enhances our understanding of their deformation mechanisms, which is crucial for optimizing their performance in technological applications.

Keywords: Ti nanoparticles, magnetron sputtering, HRTEM, dislocations

1. INTRODUCTION

Nanoobjects, defined as materials with dimensions on the nanometer scale, have revolutionized various scientific and technological fields [1, 2]. Among these, titanium (Ti) nanoparticles stand out due to their wide range of potential applications [3]. Metallic Ti particles have also been investigated for use in solar still absorber plates [4] as agents added to high-strength materials [5] or 3-D printing [6] and prosthesis production [7].Titanium is one of the most biologically inert metals, leading to its extensive use in medicine for many years [8]. It is applied as a biocompatible material in the production of implants in orthopedics, maxillofacial surgery, and neurosurgery [9]. Therefore, Ti nanoparticles are a promising candidate for medical implants and drug delivery systems.

One critical aspect of utilizing Ti nanoparticles is understanding their mechanical properties. At the nanoscale, materials often exhibit significantly different mechanical behaviors than their bulk counterparts [10, 11]. Despite the advances in the development of testing methods, research on the deformation of individual nanoparticles is limited, particularly beyond face-centered cubic (fcc) metals. Notable studies include in situ TEM examinations of silicon nanoparticles [12], as well as investigations into twinned copper [13] and silver nanoparticles [14].

Dislocation mechanisms play a vital role in defining the mechanical strength, ductility, and overall performance of nanoparticles [15]. Dislocations, which are defects within the crystal structure, influence how these nanoparticles deform and respond to external stresses. By studying these mechanisms, strategies to enhance the mechanical properties of Ti nanoparticles can be developed, making them more suitable for demanding applications. Identifying dislocations in the undeformed nanoparticles is crucial in further studies of the deformation mechanisms because they can significantly influence their mechanical behavior in the early stages of plastic deformation.

This work uses transmission electron microscopy, specifically high-resolution transmission electron microscopy, to identify dislocations inside Ti nanoparticles produced by magnetron sputtering. Energy dispersive spectroscopy is used to characterize the produced nanoparticlesfurther.

2. MATERIAL AND METHODS

The nanoparticles were prepared by magnetron sputtering from the Ti target on a glass substrate. The purity of the Ti target was 99.2%. The following conditions were used during the sputtering: pressure of 48 Pa, current of 400 mA, voltage of 164 V, and power of 66 W. The deposition process lasted for 30 minutes. Samples for TEM analysis were prepared by mixing the nanoparticle in ethanol and dripping the solution on carbon-coated TEM grids.

The produced specimens were then characterized in the transmission electron microscope JEOL JEM-2200FS using conventional transmission electron microscopy (TEM) in bright-field (BF) mode combined with high-resolution TEM (HRTEM), scanning transmission electron microscopy (STEM), and energy dispersive spectroscopy (EDS). ImageJ combined with JEMS software was used to analyze HRTEM images further.

3. RESULTS

The produced nanoparticles were characterized by STEM, as shown in **Figure 1**. The nanoparticles exhibit mostly hexagonal or less frequently round shapes, with diameters ranging from 20 to 50 nm and a mean diameter of 40 nm. The core-shell structure of the nanoparticles is evident, the EDS maps confirm the titanium core and an oxidized shell.

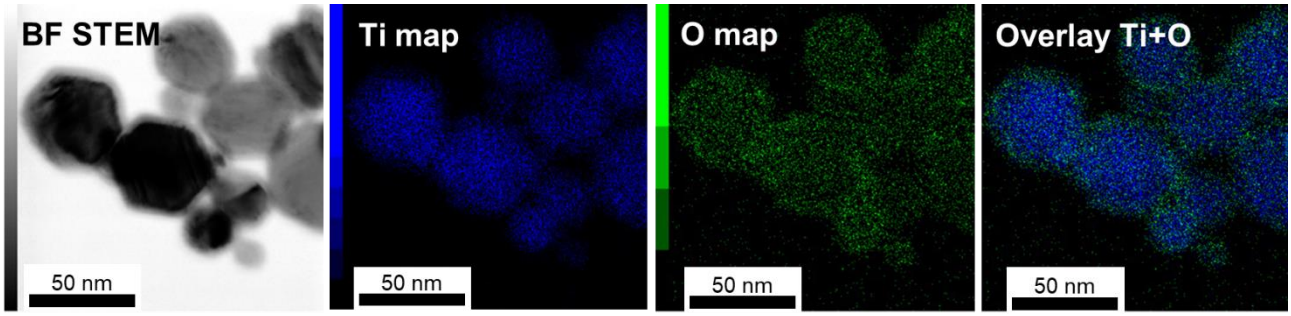

Figure 1 Ti@TiO core-shell nanoparticles, STEM BF image, and EDS maps

The TEM image of the same agglomerate is shown in **Figure 2**, with a high-resolution TEM (HRTEM) close-up provided. The Fast Fourier Transform (FFT) confirms the hexagonal close-packed (hcp) structure of titanium, with the diffractogram of the $[1\bar{2}10]$ zone axis matching the simulated diffraction pattern from JEMS. The structure matches predictions obtained by the size-temperature phase diagram of titanium nanoparticles calculated from the corresponding Gibbs free energies by Xiong et al. [16]. The diffraction pattern shows no other structures, indicating the shell is amorphous.

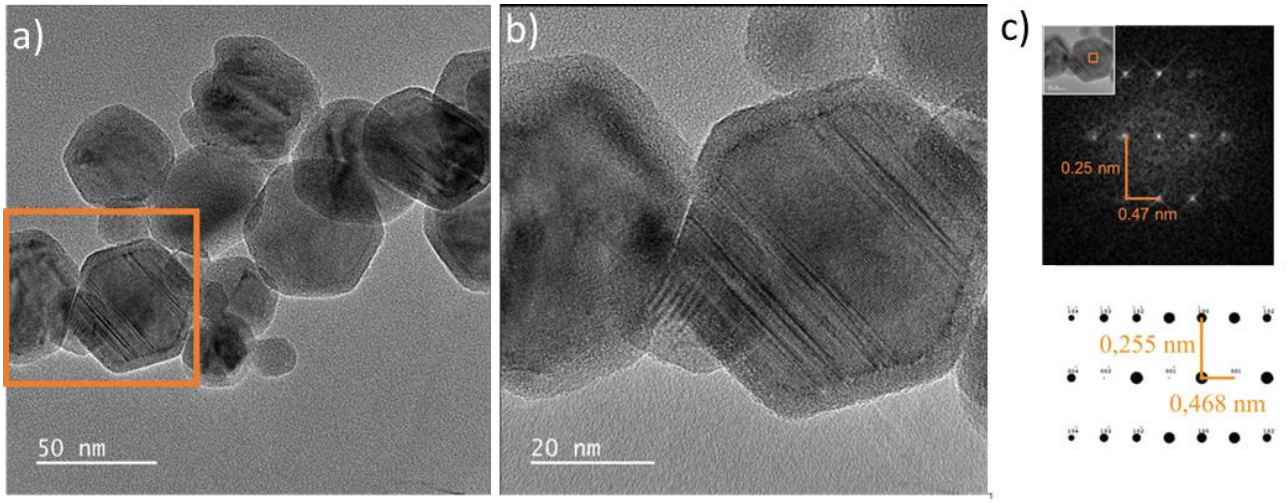

Figure 2 a) TEM BF, b) HRTEM image of the cluster of nanoparticles, c) Fast Fourier Transformation of selected area in the particle compared to Jems simulated image of hcp Ti in $[11\bar{2}0]$ orientation

In systems with hcp lattice, activation of several different slip systems is possible. Dislocations with three types of Burgers vectors, often denoted as <a>, <c>, and<a+c> types, are of primary importance [17]. The possible Burgers vectors of these types are listed in **Table 1**. In α-titanium, the primary mechanisms for deformation involve slip along three close-packed directions of the $<11\bar{2}0>$ type. These slip processes occur across different planes: the basal {0001} planes, three prismatic {1010} planes, and six pyramidal {1011} planes. The activation of dislocation motion within these slip systems is influenced by various factors, such as unit cell parameters, temperature, and crystal orientation [18].

HRTEM images of dislocations are generally challenging to analyze and require advanced approaches for simulating displacements [19]. However, certain information about the edge component is directly observable [20]. Although this method does not detect purely screw dislocations or the screw component of mixed dislocations, it allows for the determination of the Burgers vector from the edge component. To help understand HRTEM observations, it is helpful first to analyze what edge components are expected in HRTEM micrographs taken from the used zone axis. Suppose we assume that the dislocation line is parallel to the zone axis, which is the ideal case for HRTEM imaging. If the observed zone axis is $[1\bar{2}10]$, a dislocation with a Burgers vector of 1/3 $[2\bar{1}\bar{1}0]$ will appear to have an edge component of $[10\bar{1}0]$ in the HRTEM image, which is the projection of the 1/3 $[2\bar{1}\bar{1}0]$ onto the plane defined by the zone axis (**Figure 1**).Projections of all the Burgers vectors we consider for this plane are listed in **Table 2**.

Table 1 Burgers vectors in HCP system

<a> Type	<c+a> Type	<c> Type
1/3$[2\bar{1}\bar{1}0]$	1/3$[2\bar{1}\bar{1}3]$	[0001]
1/3$[\bar{1}\bar{1}20]$	1/3$[2\bar{1}\bar{1}3]$	
1/3$[\bar{1}2\bar{1}0]$	1/3$[\bar{1}\bar{1}23]$	
	1/3$[\bar{1}\bar{1}2\bar{3}]$	
	1/3$[\bar{1}2\bar{1}3]$	
	1/3$[\bar{1}2\bar{1}\bar{3}]$	

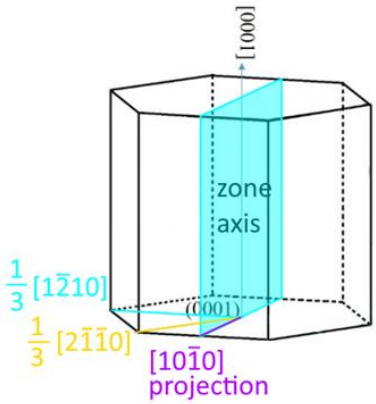

Figure 3 Projection of 1/3$[2\bar{1}\bar{1}0]$ Burgers vector to the plane perpendicular to the zone axis

Table 2 Projections of burgers vector to the zone axis $[1\bar{2}10]$

Burgers vector	Projection	Burgers vector	Projection	Burgers vector	Projection
$1/3\ [2\bar{1}\bar{1}0]$	$[10\bar{1}0]$	$1/3\ [2\bar{1}\bar{1}\bar{3}]$	$[10\bar{1}\bar{1}]$	$1/3\ [\bar{1}2\bar{1}\bar{3}]$	$[000\bar{1}]$
$1/3\ [\bar{1}\bar{1}20]$	$[\bar{1}010]$	$1/3\ [\bar{1}\bar{1}23]$	$[\bar{1}011]$	$[0001]$	$[0001]$
$1/3\ [\bar{1}2\bar{1}0]$	$[0000]$	$1/3\ [\bar{1}\bar{1}2\bar{3}]$	$[\bar{1}01\bar{1}]$		
$1/3\ [2\bar{1}\bar{1}3]$	$[10\bar{1}1]$	$1/3\ [\bar{1}2\bar{1}3]$	$[0001]$		

A better view of individual planes with noise reduction can be achieved via inverse FFT of the image. Inverse FFT images of diffraction spots from planes (0001) and $(10\bar{1}0)$ from two areas of the particle are shown in **Figure 4**. From the (0001) plane, the edge component of dislocation with projected burgers vector [0001] is visible. Both Burgers vectors 1/3 $[\bar{1}2\bar{1}3]$ of type <c+a> and [0001] of type <c> are projected in direction [0001] (**Table 1**).

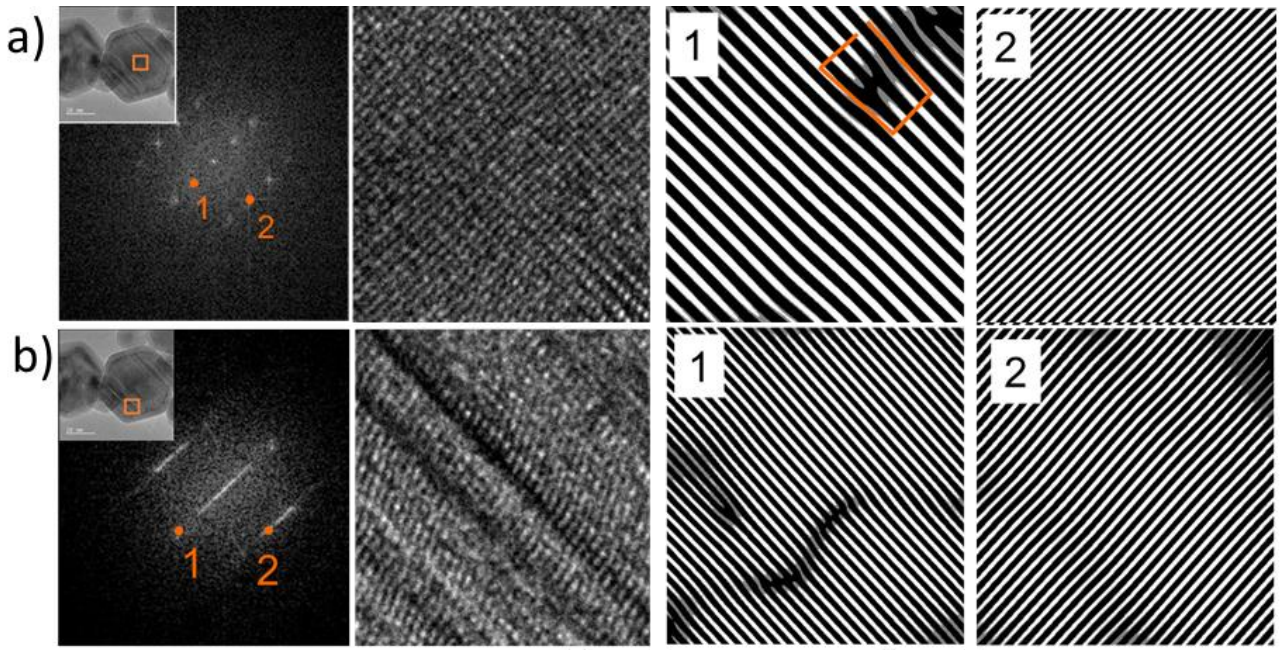

Figure 4 HRTEM image + FFT + inverse FFT in $[2\bar{1}\bar{1}0]$ zone axis: a, b) different areas of the particle

Therefore, from this orientation, they cannot be distinguished; both are possible. From the $(10\bar{1}0)$ plane, no defects could be observed. This suggests that dislocations of type <a>, the most common ones, are not present in the nanoparticle. Although dislocations with burgers vector 1/3 $[\bar{1}2\bar{1}0]$ are perpendicular to the viewed plane, the projection is zero. Therefore, they can still be present and not be observed in this orientation.

The streaks in the second FFT image indicate the presence of planar defects perpendicular to the plane of view. Since the orientation of the $(10\bar{1}0)$ planes does not change as it would in the case of twin boundaries, these are most likely thin stacking faults [21].

4. CONCLUSION

Titanium nanoparticles were successfully synthesized using a DC magnetron sputtering technique, which produced particles with a core-shell structure characterized by a titanium core and a TiO oxidized shell, as confirmed by energy dispersive spectroscopy (EDS) analysis. High-resolution transmission electron microscopy (HRTEM) revealed that the nanoparticles possess a hexagonal close-packed (hcp) crystal structure. The dislocation analysis indicated the presence of dislocations with <c> or <c+a> Burgers vectors, while no dislocations with <a> Burgers vectors were observed. Additionally, stacking faults were detected. Identifying dislocations and their types provides essential insight into initial structures that might influence the initial stages of deformation at the nanoscale.

ACKNOWLEDGEMENTS

This research was funded by the Czech Science Foundation, grant number 22-22572S.

REFERENCES

[1] MEKUYE, B., ABERA, B. Nanomaterials: An overview of synthesis, classification, characterization, and applications. *Nano Select*. 2023, vol. 4, Issue 8, pp. 486–501. https://doi.org/10.1002/nano.202300038

[2] EL-KADY, M. M., ANSARI, I., ARORA, C., RAI, N., SONI, S., VERMA, D. K., SINGH, P., MAHMOUD, A. E. D. Nanomaterials: A comprehensive review of applications, toxicity, impact, and fate to environment. *Journal of Molecular Liquids*. 2023, vol. 370, Article 121046. ISSN 0167-7322. https://doi.org/10.1016/j.molliq.2022.121046.

[3] SATO, S., YONEZAWA, T., YAMAUCHI, N., TADA, S., KOBAYASHI, Y. Synthesis of metallic titanium nanoparticles with a combination of ultrasonication and flowing of electric current. *Nano-Structures& Nano-Objects*. 2023, vol. 34, Article 100957. https://doi.org/10.1016/j.nanoso.2023.100957

[4] FAYAZ, H., RASACHAK, S., AHMAD, M. S., KUMAR, L., ZHANG, B., SELVARAJ, J., MUJTABA, M. A., SOUDAGAR, M. E. M., KUMAR, R., OMIDVAR, M. R. Improved surface temperature of absorber plate using metallic titanium particles for solar still application. *Sustainable Energy Technologies and Assessments*. 2022, vol. 52, Article 102092.

[5] LIU, X. Q., LI, C. J., YOU, X., XU, Z. Y., LI, X., BAO, R., TAO, J. M., YI, J. H. Size-dependent effects of Ti powders in the pure aluminum matrix composites reinforced by carbon nanotubes. *Journal of Alloys and Compounds*. 2020, vol. 823, Article 153824.

[6] GUO, A. X. Y., CHENG, L., ZHAN, S., ZHANG, S., XIONG, W., WANG, Z., WANG, G., CAO, S. C. Biomedical applications of the powder-based 3D printed titanium alloys: A review. *Journal of Materials Science & Technology*. 2022, vol. 125, pp. 252-264.

[7] PRANANINGRUM, W., TOMOTAKE, Y., NAITO, Y., BAE, J., SEKINE, K., HAMADA, K., ICHIKAWA, T. Application of porous titanium in prosthesis production using a moldless process: Evaluation of physical and mechanical properties with various particle sizes, shapes, and mixing ratios. *Journal of the Mechanical Behavior of Biomedical Materials.* 2016, vol. 61, pp. 581-589.

[8] KURAPOV, Y. A., LITVIN, S. E., BELYAVINA, N. N. et al. Synthesis of pure (ligandless) titanium nanoparticles by EB-PVD method. *Journal of Nanoparticle Research*. 2021, vol. 23, Article 20. https://doi.org/10.1007/s11051-020-05110-3

[9] BHAGYARAJ, S. M., OLUWAFEMI, O. S., KALARIKKAL, N., THOMAS, S. (Eds.). *Synthesis of Inorganic Nanomaterials: Advances and Key Technologies*. 2018, Elsevier Ltd. https://doi.org/10.1016/C2016-0-01718-7

[10] GLEITER, H. *Progress in Materials Science*. 1989, vol. 33, pp. 223.

[11] MORDEHAI, D., LEE, S. W., BACKES, B., SROLOVITZ, D. J., NIX, W. D., RABKIN, E. Size effect in compression of single-crystal gold microparticles. *Acta Materialia*. 2011, vol. 59, pp. 5202-5215. https://doi.org/10.1016/j.actamat.2011.04.057

[12] DENEEN, J., MOOK, W. M., MINOR, A., GERBERICH, W. W., CARTER, C. B. Fracturing a nanoparticle. *Philosophical Magazine*. 2007, vol. 87, Page 29.

[13] CASILLAS, G., PALOMARES-BÁEZ, J. P., RODRÍGUEZ-LÓPEZ, J. L., LUO, J., PONCE, A., ESPARZA, R., JOSÉ-YACAMAN, M. In situ TEM study of mechanical behaviour of twinned nanoparticles. *Philosophical Magazine*. 2012, vol. 92, Issue 35, pp. 4437–4453. https://doi.org/10.1080/14786435.2012.709951

[14] CARLTON, C. E., FERREIRA, P. J. In situ TEM nanoindentation of nanoparticles. *Micron*. 2012, vol. 43, Issue 11, pp. 1134-1139. https://doi.org/10.1016/j.micron.2012.03.002

[15] GARCIA VIDADLE, G., GONZALEZ, R. I., VALENCIA, F. J., AMIGO, N., TRAMONTINA, D., BRINGA, E. M. Simulations of plasticity in diamond nanoparticles showing ultrahigh strength. *Diamond and Related Materials*. 2022, vol. 126, Article 109109. https://doi.org/10.1016/j.diamond.2022.109109

[16] XIONG, S., et al. Size- and temperature-induced phase transformations of titanium nanoparticles. *EPL (Europhysics Letters)*. 2011, vol. 93, Article 66002.

[17] AUBRY, S., RHEE, M., HOMMES, G., BULATOV, V. V., ARSENLIS, A. Dislocation dynamics in hexagonal close-packed crystals. *Journal of the Mechanics and Physics of Solids*. 2016, vol. 94, pp. 105-126. https://doi.org/10.1016/j.jmps.2016.04.019.

[18] LI, Y., PO, G., CUI, Y., GHONIEM, N. Prismatic-to-basal plastic slip transition in zirconium. *Acta Materialia*. 2023, vol. 242, Article 118451. https://doi.org/10.1016/j.actamat.2022.118451

[19[LAY, S. HRTEM investigation of dislocation interactions in WC. *International Journal of Refractory Metals and Hard Materials*. 2013, vol. 41, pp. 416-421. https://doi.org/10.1016/j.ijrmhm.2013.05.017

[20] CHENG, G. M., XU, W. Z., JIAN, W. W., et al. Dislocations with edge components in nanocrystalline bcc Mo. *Journal of Materials Research*. 2013, vol. 28, pp. 1820–1826. https://doi.org/10.1557/jmr.2012.403

[21] SUN, Q., ZHANG, Q., LI, B., ZHANG, X., TAN, L., LIU, Q. Non-dislocation-mediated basal stacking faults inside {101-1} twins. *Scripta Materialia*. 2017, vol. 141, pp. 85-88. https://doi.org/10.1016/j.scriptamat.2017.07.036